Relationships between Tumor Size and Curability for Uniformly Targeted Therapy with Beta-Emitting Radionuclides

J.A. O'Donoghue, M. Bardiès and T.E. Wheldon

Departments of Radiation Oncology and Clinical Physics, University of Glasgow, Glasgow, United Kingdom; and Groupe Biophysique-Cancérologie, INSERM U211, Institut de Biologie, Nantes, France

Targeted radionuclide therapy is a new form of radiotherapy that differs in some important respects from external beam irradiation. One of the most important differences is due to the finite range of ionizing beta particles emitted as a result of radionuclide disintegration. The effects of particle range have important implications for the curability of tumors. **Methods:** We used a mathematical model to examine tumor curability and its relationship to tumor size for 22 beta-emitting radionuclides that may have therapeutic potential. The model assumed a uniform distribution of radionuclide throughout. **Results:** For targeted radionuclide therapy, the relationship between tumor curability and tumor size is different from that for conventional external beam radiotherapy. With targeted radionuclides, there is an optimal tumor size for cure. Tumors smaller than the optimal size are less vulnerable to irradiation from radionuclides because a substantial proportion of the disintegration energy escapes and is deposited outside the tumor volume. **Conclusion:** We found an optimal tumor size for radiocurability by each of the 22 radionuclides considered. Optimal cure diameters range from less than 1 mm for short-range emitters such as ^{199}Au and ^{33}P to several centimeters for long-range emitters such as ^{90}Y and ^{188}Re. The energy emitted per disintegration may be used to predict optimal cure size for uniform distributions of radionuclide.

Key Words: targeted radionuclide therapy; radioimmunotherapy; tumor curability; heterogeneity

J Nucl Med 1995; 36:1902–1909

Targeted radionuclide therapy involves the use of radiolabeled tumor-seeking molecules to deliver a cytotoxic dose of radiation to tumor cells. Although not generally applicable in cancer treatment at present, targeted radionuclide therapy is beginning to be useful in the treatment of some tumor types (*1–4*).

The main theoretic advantage of targeted radionuclide therapy is that radiation can be delivered selectively to subclinical tumors and metastases that are too small to be imaged and thereby treated by surgical excision or local external beam radiotherapy (XRT). In addition, the absorbed doses to tumors achieved by targeting may be higher than can be delivered by systemic XRT (i.e., total body irradiation).

For any radiation-based therapy, the likelihood of tumor cure depends on three factors.

1. The radiation dose absorbed in the tumor and its pattern of delivery (e.g., dose rate and fractionation).
2. The number of clonogenic tumor cells present. These all have to be sterilized to cure the tumor.
3. The response of the tumor cells to radiation (e.g., radiosensitivity, repair capacity and proliferation rate).

These factors are as important in targeted radionuclide therapy as they are in conventional XRT. The main differences between targeted radiotherapy and XRT are caused by dosimetry, with dose-rate effects a secondary factor. In XRT, a geometric target volume is defined, and overlapping radiation fields are arranged to treat this volume as uniformly as possible. Any tumor within the target volume receives a near-uniform radiation dose, independent of its size (a microscopic tumor within the target volume will receive the same dose as a bulk tumor). This is because the tumor itself does not determine the absorption of radiation energy, which is dependent only on the flux of ionizing particles produced by the overlapping radiation fields.

For targeted radiotherapy, the situation is different. In this case, the absorbed radiation dose is due to the flux of ionizing particles produced by radionuclides distributed within or around the tumor. The distribution of radionuclide depends on the biologic properties of the tumor. Factors such as the affinity of targeting molecules for the tumor cells and the extent and permeability of the tumor vasculature determine the intratumor distribution of targeting molecules. The physical characteristics of the radionuclides delivered by the targeting molecules imposes a further level of variability. Important in this respect is the energy spectrum of the ionizing particles, which determines the range of the energy emission. The distribution of radiation dose throughout a tumor depends on tumor size, the radionuclide in use and its intratumor distribution. This

Received Mar. 30, 1994; revision accepted Aug. 22, 1994

For correspondence or reprints contact: J. A. O'Donoghue, PhD, Department of Radiation Oncology, University of Glasgow, CRC Beatson Laboratories, Garscube Estate, Bearsden, Glasgow G61 1BD, UK.

TABLE 1
Potential Therapeutic Radionuclides Examined

Radionuclide	$T_{1/2}$ (days)	E_{total} (keV)	Δ (g Gy/MBq day)
^{32}P	14.28	695.5	9.615
^{33}P	25.4	76.6	1.059
^{47}Sc	3.35	162.6	2.247
^{67}Cu	2.58	154.1	2.131
^{77}As	1.62	226.4	3.130
^{90}Y	2.67	939.1	12.98
^{105}Rh	1.47	153.5	2.121
^{109}Pd	0.56	436.6	6.035
^{111}Ag	7.45	350.9	4.852
^{121}Sn	1.13	114.5	1.583
^{131}I	8.02	192.3	2.658
^{142}Pr	0.80	809.3	11.19
^{143}Pr	13.57	315.4	4.360
^{149}Pm	2.21	358.9	4.961
^{153}Sm	1.95	269.1	3.720
^{159}Gd	0.77	310.1	4.286
^{166}Ho	1.12	694.5	9.601
^{177}Lu	6.71	146.7	2.028
^{186}Re	3.78	340.8	4.711
^{188}Re	0.71	778.3	10.76
^{194}Ir	0.80	802.0	11.09
^{199}Au	3.14	142.4	1.969

E_{total} = mean energy emitted per disintegration in the form of beta particles and electrons; Δ = mean energy emitted per unit cumulated activity, i.e., the equilibrium dose constant.

complex situation results in a heterogeneous distribution of radiation dose, which is relatively high in some intratumoral regions, although others experience reduced levels. In the simplest case of a uniform distribution of radionuclide throughout a tumor volume, when the tumor is large in comparison to the range of the ionizing particles, most of the energy is absorbed within the tumor. In cases in which the tumor dimensions are smaller than the range, a large proportion of the energy can escape (*5*).

Only a few radionuclides have been used in clinical practice (primarily ^{131}I and, to a lesser extent, ^{90}Y), but a much larger number have potential application. The choice of therapy radionuclides and the relative advantages of one compared with another have been discussed (*5,6*). Recently, Mausner and Srivastana (*7*) listed 18 beta-emitting radionuclides that have potential therapeutic use.

In this paper, we examine how the choice of radionuclide therapy influences the relationship between tumor curability and tumor size. Specifically, the 18 radionuclides listed by Mausner and Srivastana (*7*) with the addition of four others (^{32}P, ^{33}P, ^{121}Sn and ^{143}Pr) are considered, making a total of 22 (Table 1). These radionuclides have a variety of emission spectra and half-lives, and not all are equally available or convenient; however, this latter aspect of radionuclide choice is not considered here. Only the simplest case for the intratumor distribution of radionuclide (uniform throughout the tumor volume) is examined.

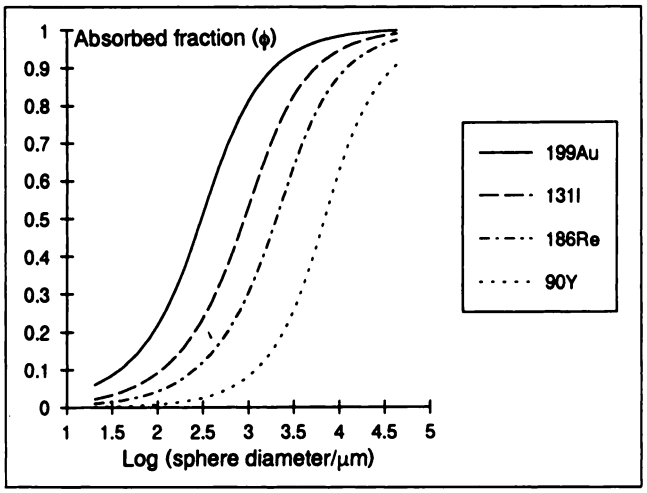

FIGURE 1. Relationship between absorbed fraction of disintegration energy, ϕ, and sphere diameter for four radionuclides for a uniform volume distribution [data from Bardiès and Chatal (*8*)].

MATERIALS AND METHODS

Overview

The relationships between tumor size and curability were examined with a mathematic model. There are essentially two parts to this.

1. The first part is the calculation of absorbed dose fractions for the 22 radionuclides for uniform volume distributions of radionuclide within spheres of varying size.
2. The absorbed fractions are incorporated into a model of tumor cure that takes into account tumor cell radiosensitivity and proliferation.

Calculation of Absorbed Fractions

Absorbed fractions (ϕ) were calculated for spheres that ranged in diameter from 20 μm to 4.4 cm. The details of the computational procedure used have been reported elsewhere (*8*). Briefly, absorbed fractions for monoenergetic electrons were calculated with point source kernels and integration over the volume of the sphere. These were then used to calculate absorbed fractions for radionuclides by integration over beta-spectra generated by the computer code SPEBETA (*9*). Figure 1 shows the relationship between ϕ and sphere diameter for a selection of four of the radionuclides considered. It is apparent that the limiting value of ϕ is 1 for a volume distribution. This means that as the sphere becomes very large in comparison to the radionuclide emission range, almost all the energy is absorbed when the radionuclide is evenly distributed throughout the volume.

Model of Tumor Curability

The model of tumor curability was based on a spheric tumor composed of a population of tumor cells, also taken to be spheric, and an intercellular matrix of unit density material. The tumor cells were assumed to all have the same radiobiologic properties in terms of radiosensitivity and proliferation rate. A proportion, ψ, was taken to be clonogenic. The specific assumptions of the model are as follows.

1. The number of tumor cells, N, in a tumor of diameter, d, is given by:

$$N = q(d/d_c)^3, \qquad \text{Eq. 1}$$

where q is a packing factor equal to the proportion of the tumor volume composed of tumor cells and d_c is the diameter of a tumor cell. The number of clonogenic tumor cells, η, is ψN where ψ is the clonogenic fraction, which was taken to be constant throughout the tumor size range.

2. The radiation dose rate, r(t), experienced by the tumor cells is assumed to decay monoexponentially.

$$r(t) = r_0 \exp(-kt), \quad \text{Eq. 2}$$

where r_0 is the initial dose rate and k is the effective decay constant. This means the initial phase of accumulation of radionuclide into the tumor is ignored. The effective half-life T_{eff} and k are related by

$$k = \ln 2/T_{eff} \quad \text{Eq. 3}$$

and the physical, T_{phys}, and biologic, T_{biol}, half-lives are related to T_{eff} by

$$T_{eff} = T_{phys}T_{biol}/(T_{phys} + T_{biol}) \quad \text{Eq. 4}$$

3. The initial dose rate, r_0, in the tumor is given by

$$r_0 = C_0\Delta\phi, \quad \text{Eq. 5}$$

where C_0 is the initial activity per unit mass of tumor, Δ is the mean energy emitted in the form of beta particles and electrons per unit cumulated activity and ϕ is the absorbed fraction. For any particular size of tumor, both Δ and ϕ are radionuclide dependent; ϕ is also tumor size dependent.

4. The differential equation that governs the rate of change of the number of clonogenic tumor cells, η, is

$$\frac{d\eta}{dt} = -\alpha r(t) + \lambda\eta, \quad \text{Eq. 6}$$

where α is the radiosensitivity in reciprocal Grays and λ is the proliferation rate, related to T_D, the population doubling time, by

$$\lambda = \ln 2/T_D \quad \text{Eq. 7}$$

Equation 6 means that the rate of tumor cell kill is directly proportional to the dose rate and that exponential proliferation of surviving tumor cells takes place during the irradiation process. For this situation, the minimum value of surviving fraction of clonogenic tumor cells, S_{min} is given by the following (*10*).

$$S_{min} = \exp(-\alpha ED), \quad \text{Eq. 8}$$

where E is the therapeutic efficiency, which takes account of the amount of radiation dose that is wasted because of tumor cell proliferation. When r_0 is greater than λ/α, E is given by

$$E = 1 - \frac{\lambda}{\alpha r_0}\left\{1 - \ln\left(\frac{\lambda}{\alpha r_0}\right)\right\} \quad \text{Eq. 9}$$

Otherwise, E = 0.

D is the total cumulated radiation dose given by

$$D = \int_0^\infty r_0 \exp(-kt)\,dt = \frac{r_0}{k} \quad \text{Eq. 10}$$

TABLE 2
Numeric Values for the Model Parameters*

Parameter	Base value	Limits of variability
Tumor cell diameter, d_c	20 μm	Fixed
Clonogenic fraction, ψ	0.1	0.01–1.0
Packing factor, q	0.4	Fixed
Radiosensitivity, α	0.5 Gy^{-1}	0.2–1.0
Biological half-life, T_b	2 days	1–4
Tumor population doubling time, T_D	4 days	1–20

*The baseline values were used in the calculation of central estimates of optimal tumor cure size, including the derivation of Figures 2 and 3. The parameters were allowed to vary up to the limits shown to gain an impression of the stability of the optimal size estimates.

5. The expectation value of the minimum number of clonogenic tumor cells produced by targeted radionuclide therapy, η_{min} is ψNS_{min} from assumptions 1 and 4. The probability of tumor cure, P_c, is taken to be the probability that the number of clonogenic tumor cells reaches zero at its minimum value. This is equal to the first term of the Poisson distribution with mean η_{min}.

$$P_c = \exp(-\eta_{min}) \quad \text{Eq. 11}$$

It is now possible to write an explicit equation for the probability of tumor cure in terms of the primary parameters.

$$P_c = \exp\left\{-\psi q(d/d_c)^3 \exp\left(-\frac{\alpha C_0\Delta\phi}{\ln 2\left(\frac{T_{phys}+T_{biol}}{T_{phys}T_{biol}}\right)}\right)\cdot\left\{1-\frac{\ln 2}{\alpha C_0\Delta\phi T_D}\left(1-\ln\left(\frac{\ln 2}{\alpha C_0\Delta\phi T_D}\right)\right)\right\}\right\} \quad \text{Eq. 12}$$

Numeric Data Used in the Calculations

Cure probabilities were calculated for tumors with diameters in the range from 200 μm to 4.4 cm with values of ϕ for a uniform volume distribution of radionuclide. The appropriate values of Δ and T_{phys} were used for each radionuclide. The baseline values of the parameters ψ, d_c, α, T_{biol} and T_D are shown in Table 2. These particular numeric values were chosen as follows.

1. A clonogenic fraction, ψ, of 0.1 corresponds to 1 tumor cell in 10 being capable of giving rise to an indefinitely proliferating tumor clone. This is an approximation. In general, it would be anticipated that the clonogenic fraction would be greatest for smaller tumors, which tends toward the limiting value of 1.0 for a tumor that contains one cell.
2. The diameter of a tumor cell, d_c, was taken as 20 μm. This is an approximation that corresponds to a typical tumor cell diameter.
3. The radiosensitivity value, α, of 0.5 Gy^{-1} is representative of the in vitro behavior of a category of "radiosensitive" tumors such as lymphoma, as described by Fertil and Malaise (*11*).
4. A biologic half-life of 2 days is broadly representative of the tumor clearance of targeting radiopharmaceuticals.

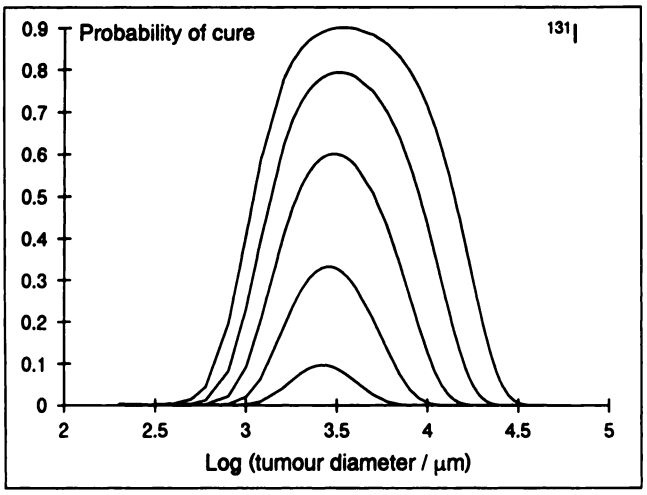

FIGURE 2. Relationship between tumor cure probability and tumor size for a uniform volume distribution of ^{131}I calculated with baseline model parameter values as described in the text and shown in Table 2. Different curves correspond to different levels of tumor-bound radionuclide. Peak in curability occurs at a diameter of 3.4 mm.

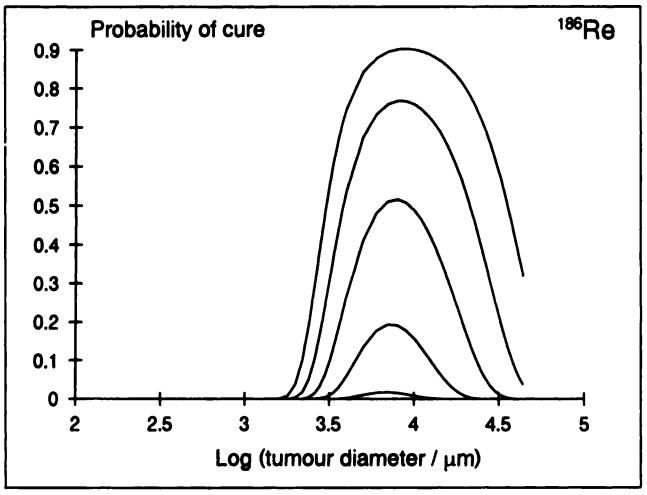

FIGURE 3. Tumor cure probability versus tumor size for ^{186}Re. Maximum cure probability occurs at a diameter of 9 mm.

5. Finally, a doubling time of 4 days is an estimate of a typical intermitotic interval for exponentially proliferating tumor cells.

Although these numeric values are reasonable, it is very important that, in a mathematic modeling study such as this, the conclusions be robust and not critically dependent on the numeric values chosen for these parameters. In any one particular patient-tumor-site scenario, tumor cells will have specific values appropriate to their intrinsic nature and environment; however, these values are unlikely to be known in advance to any accuracy. For this reason, the parameter estimates were allowed to vary from the above baseline values, as shown in Table 2. Clonogenic fraction was allowed to vary between 0.01 and 1.0. Radiosensitivity was varied between 0.2 and 1.0 Gy^{-1}, which encompassed the range from radioresistant (*11*) to highly radiosensitive (*12*). Biologic half-life and tumor doubling time were varied between 1 and 4 days and 1 and 20 days, respectively, which encompassed all likely scenarios. In all cases, combinations of parameter values that produced extreme results were chosen to derive as robust a conclusion as possible.

The initial activity per unit mass of tumor, C_0, was found by iteration for each calculation run to produce a maximum cure probability of 0.90. The initial number of radionuclide atoms per unit mass, R_0, is related to C_0 by $R_0 = C_0 \times (T_{phys}/\ln 2)$. This quantity was used to compare different radionuclides in terms of the number of bound atoms required to produce similar cure probabilities in the tumor size range of optimal efficiency.

RESULTS

Relationship between Tumor Size and Curability

Figures 2 and 3 show a set of curves of tumor cure probability as a function of tumor size for the radionuclides ^{131}I and ^{186}Re, respectively. These are taken as examples to illustrate the general features of the relationships. The cure curves for all the other radionuclides are qualitatively similar, although quantitatively the peak in cure probability appears at different tumor diameters. Each curve corresponds to a different value of initial activity per unit mass, C_0, with greater values toward the top. The values of C_0 that produce a maximum cure probability of 0.9 are shown in Table 3 together with the corresponding values of R_0. Figure 2 shows that there is a maximum value of curability that occurs at a diameter of approximately 3.4 mm for ^{131}I. For ^{186}Re, the maximum curability occurs at a tumor diameter of approximately 9 mm, as shown by Figure 3. It is apparent that, over the size range considered here, the probability of curing tumors smaller than the optimal diameter decreases progressively with decreasing size. The optimal cure diameters for all 22 radionuclides are shown in Table 3.

Dependence of Optimal Cure Sizes on Model Parameters

The numeric values of the model parameters were varied, as described in the Materials and Methods section. Figure 4 shows for ^{131}I the cure probability curves for the parameter combinations, which produce the minimum and maximum value of optimal cure size. These values are d_{min} = 2.6 mm and d_{max} = 5.0 mm. The optimal cure size range for ^{131}I is thus (2.6–5.0 mm). The same procedure was adopted for all the radionuclides examined and the summary of optimal cure size ranges is shown in Table 3.

Relationship between Optimal Cure Size and Mean Energy Emitted per Disintegration

The central estimates of the optimal cure size for each radionuclide were plotted against the mean energy emitted per disintegration in the form of beta particles and electrons. This was fitted by linear regression analysis (adjusted $r^2 = 0.98$). The regression equation is $D_{opt} = 0.039\ E_{total} - 4$, where D_{opt} is in millimeters and E_{total} is in kiloelectron volts and is shown in Figure 5 together with the 95% confidence curves for the regression line and for individual values.

TABLE 3
Values of Initial Activity (C_0) and Number of Bound Radionuclide Atoms (R_0) per Gram Required to Produce a Cure Probability of 0.9 at the Optimal Size*

Radionuclide	C_0 (MBq/g)	R_0 (1/g)	Optimal diameter (mm)	Optimal range (mm)
^{32}P	2.08	3.71×10^{12}	22.0	18.0–30.0
^{33}P	10.3	3.26×10^{13}	0.6	<0.2–1.0
^{47}Sc	9.07	3.79×10^{12}	2.6	2.0–3.8
^{67}Cu	10.1	3.24×10^{12}	2.0	1.6–2.8
^{77}As	9.71	1.96×10^{12}	5.0	3.6–6.0
^{90}Y	2.43	8.09×10^{11}	34.0	28.0–42.0
^{105}Rh	13.9	2.56×10^{12}	2.8	2.0–3.6
^{109}Pd	10.7	7.50×10^{11}	7.0	6.0–9.0
^{111}Ag	4.07	3.79×10^{12}	9.0	7.0–13.0
^{121}Sn	19.3	2.72×10^{12}	1.6	1.0–2.0
^{131}I	6.37	6.38×10^{12}	3.4	2.6–5.0
^{142}Pr	5.37	5.35×10^{11}	28.0	24.0–34.0
^{143}Pr	4.05	6.86×10^{12}	8.0	6.0–11.0
^{149}Pm	5.86	1.61×10^{12}	9.0	8.0–12.0
^{153}Sm	7.27	1.77×10^{12}	3.8	2.8–5.0
^{159}Gd	12.0	1.15×10^{12}	7.0	6.0–9.0
^{166}Ho	4.83	6.75×10^{11}	21.0	18.0–25.0
^{177}Lu	7.92	6.63×10^{12}	2.0	1.2–3.0
^{186}Re	4.97	2.34×10^{12}	9.0	7.0–12.0
^{188}Re	6.03	5.34×10^{11}	26.0	23.0–32.0
^{194}Ir	5.43	5.41×10^{11}	28.0	24.0–34.0
^{199}Au	8.66	3.39×10^{12}	0.8	0.4–1.2

*Also shown are the central estimates of optimal tumor diameters for curability derived from the baseline parameter estimates together with optimal tumor diameter ranges generated by variation in the numeric parameters, as described in the text.

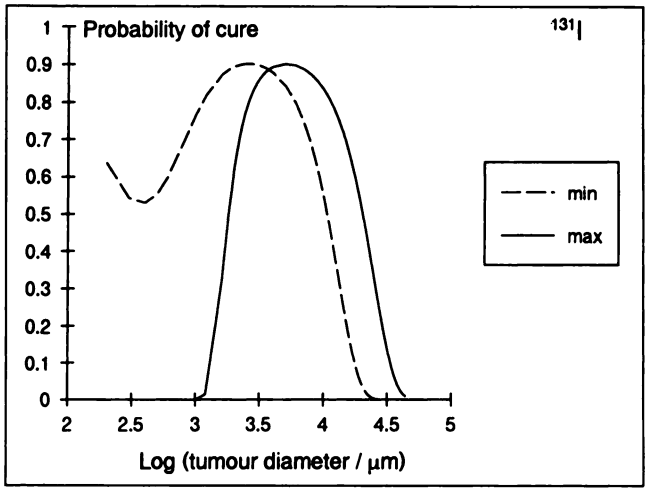

FIGURE 4. Numeric values of model parameters were varied in such a way as to either minimize or maximize optimal cure diameter. Iodine-131 was used. Minimum optimal diameter was 2.6 mm and maximum was 5.0 mm. This procedure was adopted for all radionuclides studied, and resultant ranges of optimal diameter are shown in Table 3.

Number of Bound Radionuclide Atoms Required for Tumor Cure

As described in the Materials and Methods section, the initial number of bound radionuclide atoms per unit mass, $R_0 = C_0 \times (T_{phys}/\ln 2)$, where C_0 is the initial bound activity per unit mass and T_{phys} is the physical half-life. The values of C_0 that produced a 90% cure probability were evaluated during the course of the optimal cure size calculations. Figure 6 plots the relationship between R_0 (90% cure) and the composite quantity (T_{phys}/E_{total}). The data point corresponding to the radionuclide ^{33}P ($R_0 = 3.3 \times 10^{13}$: (T_{phys}/E_{total}) = 0.33) has been omitted from this set because of its undue influence. The data conform to a linear relationship (adjusted $r^2 = 0.98$) with the regression equation $R_0 = 7 \times 10^{11} + 1.4 \times 10^{14}$ (T_{phys}/E_{total}), where T_{phys} is in days.

DISCUSSION

Shapes of Tumor Curability Compared with Size Curves

For targeted radionuclide therapy, the shapes of the curves that relate tumor curability to tumor size (Figs. 2 and 3) are radically different from those for XRT. Figure 7 shows the corresponding relationship for XRT given as a single dose. In this case, there is no optimal cure size, only a progressively decreasing likelihood of cure as the tumor size increases. In this simple model, this is due to the effect of increasing cell number. As the radiation dose gets larger, the likelihood of tumor cure increases and it becomes possible to cure larger tumors.

For targeted radiotherapy, the relationship between cure and size is essentially the same for tumors larger than the optimal size, as it is in the case of XRT. In this part of the curve, the dominant mechanism is the increase in clonogenic cell number, which leads to a reduction in cure probability as the tumor increases in size. The main difference occurs for tumors smaller than the optimal size. Here the dominant mechanism is the reduction in the ability of tumors to absorb the radiation energy emitted by bound

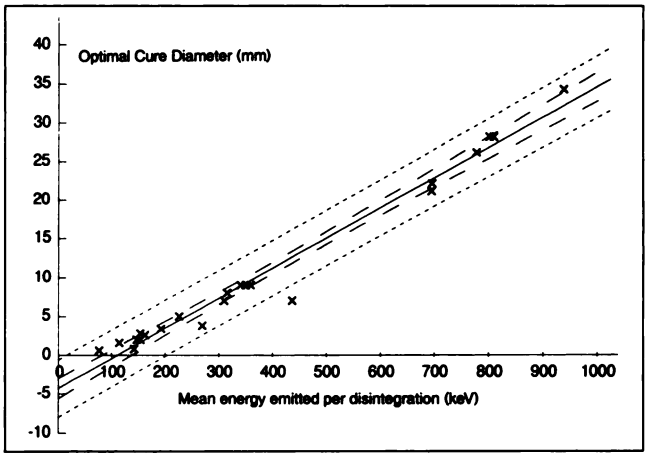

FIGURE 5. Relationship between optimal cure diameter and mean energy emitted per disintegration. Linear regression was fitted to these data, which yielded a regression equation of $D_{opt} = 0.039 E_{total} - 4$ (adjusted $r^2 = 0.98$); 95% confidence curves for regression line and for individual points are also shown. Mean disintegration energy may be used to predict optimal cure size.

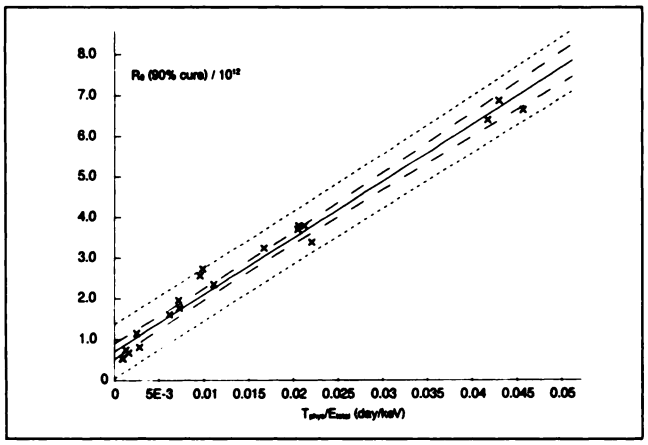

FIGURE 6. Relationship between R_0, the number of radionuclide atoms bound per unit mass, which is required to produce a cure probability of 90% at optimal cure size for baseline parameter estimates, and ratio (T_{phys}/E_{total}). This was fitted by linear regression analysis to yield a regression equation

$$R_0 = 7\times10^{11} + 1.4\times10^{14}\left(\frac{T_{phys}}{E_{total}}\right) \text{(adjusted } r^2 = 0.98\text{)}$$

One data point (corresponding to ^{33}P) was omitted from this set because it was unduly influential (3.3×10^{13}, 0.33); 95% confidence curves for regression line and for individual points are also shown.

radionuclides with decreasing size. Tumors in this category are operationally resistant to targeted radiotherapy. The optimal cure size corresponds to a point where there is a balance between the two competing mechanisms. The requirement for increasing radiation dose to cure larger tumors is independent of the radionuclide being used. However, the fall off in energy absorption is related to the range of the beta particles emitted and therefore varies between radionuclides. It is therefore this mechanism that gives rise to the radionuclide-specific differences in optimal cure size.

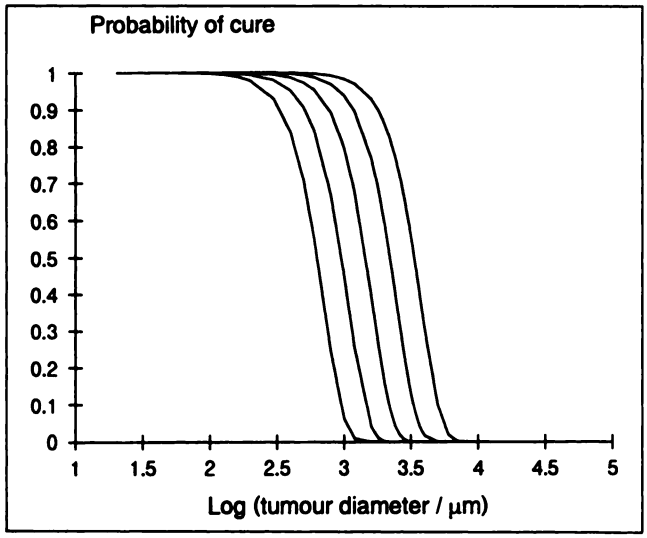

FIGURE 7. Relationship between tumor cure probability and tumor size for single exposure to XRT. Different curves correspond to different doses. Smaller tumors are more easily cured than larger ones, which contrasts with situation for targeted radionuclides, as shown in Figures 2 and 3.

The prediction that cure probability decreases with size for tumors smaller than the optimal diameter has been tested experimentally (*13*). In that study, [^{131}I]metaiodobenzylguanidine (MIBG) was used to treat neuroblastoma spheroids of two different sizes (250 and 400 μm in diameter). With both regrowth delay and spheroid cure as end points, the reduced vulnerability of smaller spheroids to targeted radionuclide therapy was confirmed.

Effects of Varying Model Parameters on Optimal Cure Size

The numeric values of the model parameters were varied, as shown in Table 2, to investigate the stability of the optimal cure sizes. Figure 4 illustrates the difference in optimal diameter produced when the extreme combinations for ^{131}I are chosen. In several trials, the dominant factor in determining optimal cure size was found to be the clonogenic cell density. This is a composite quantity depending on ψ, the clonogenic fraction, q, the geometric packing factor and d_c, the tumor cell diameter, but was varied in the model only by adjustment of the value of ψ. The optimal cure size increases as clonogenic cell density increases. The next most dominant factor was T_D, the population doubling time (optimal cure size decreases as T_D increases), and finally T_{biol}, the biologic half-life (optimal cure size increases as T_{biol} increases). Although the absolute value of cure probability depends critically on the radiosensitivity, α, the optimal cure size is insensitive to this parameter.

As described in the Materials and Methods Section, it is important that the model findings are robust and not critically dependent on the values of biologic parameters. Variations in these parameters alter the calculated values of optimal cure size, but, as can be seen from Table 3, the optimal ranges are fairly narrow, which indicates that the findings are indeed robust. What this means in practice is that the optimal cure size is somewhere within the calculated range. The actual value will depend on such factors as clonogenic cell density, proliferation rate and radionuclide clearance kinetics in the fashion described above.

Relationship between Emission Energy and Optimal Cure Size

Figure 6 shows that the relationship between the mean energy emitted per disintegration and the central estimate of optimal cure diameter is fairly close to linear. It is therefore possible to use the quantity E_{total} as a predictor for optimal cure size. The regression equation is

$$D_{opt} = 0.039\ E_{total} - 4 \qquad \text{Eq. 13}$$

where D_{opt} is in millimeters and E_{total} is in kiloelectron volts.

As discussed above, the optimal size is determined by competition between energy absorption and clonogenic cell number. This tends to have its most favorable balance

in the region where the absorbed fraction, ϕ, is in transition from a steep increase to a more shallow approach to its limiting value. On average, optimal cure sizes occur at ϕ = 0.85 (±0.06, 95% confidence interval) with lower values of ϕ corresponding to smaller optimal sizes.

Number of Radionuclide Atoms Bound to Tumor

The number of radionuclide atoms, R_0 which must be bound to the tumor per unit mass to produce a cure probability of 0.9 at the optimal tumor diameter, gives an impression of relative targeting effectiveness.

In this regard, the key parameters are the T_{phys} and the energy spectrum of the emissions. Together, these give an indication of the radiation dose rate produced in equilibrium conditions for any particular concentration of radionuclide atoms. If the number of radionuclide atoms per unit mass is C_0 and the energy emitted per disintegration is E_{total}, then the energy emitted per unit time, ε, is given by

$$\varepsilon = \frac{E_{total}}{T_{phys}} C_0 \ln 2 \qquad \text{Eq. 14}$$

where T_{phys} is the physical half-life.

This quantity is, of course, directly proportional to the dose rate. The ratio E_{total}/T_{phys} is therefore a useful indicator of the potency of the radionuclide.

This is supported by Figure 6, which plots R_0 against the ratio T_{phys}/E_{total}. These data conform to a linear relationship. The calculated values of R_0 are highly dependent on the assumed value of radiosensitivity, α, and are therefore only of use in radionuclide intercomparison in a relative sense. For any particular value of radiosensitivity, the corresponding estimates of R_0 constitute a lower limit on what would be required clinically. In reality, the existence of regions of reduced uptake, or cold spots, would mean that substantially higher numbers of bound radionuclide atoms would probably be necessary for a useful therapeutic effect.

Study Limitations

In this model study, only the simplest scenario of a uniform distribution of beta-emitting radionuclide throughout a tumor volume has been considered. No attempt has been made to consider other radionuclide configurations, such as surface or diffusion gradient distributions. These distributions are likely to apply to many clinical scenarios, including that of metastatic ovarian carcinoma treated by intraperitoneal infusion of radioimmunoconjugates (*14*). In addition, the effects of heterogeneity of radionuclide uptake such as cold spots has not been addressed. To examine these complicating factors, a model of a tumor as a single entity is inappropriate, and a multicompartmental model would be required. The authors intend to investigate this approach in the future.

Even for the situation of a uniform volume distribution, it is apparent that the implications of the size-cure relationships can be rather complicated. Some of the results described above depend on the assumed values of the model parameters. These include derived values of C_0 and R_0, the activity and number of radionuclide atoms, respectively, required per unit mass to give a 90% cure probability at the optimal cure size. The calculated ranges of optimal cure size, however, are fairly robust because they were derived from a wide range of parameter values.

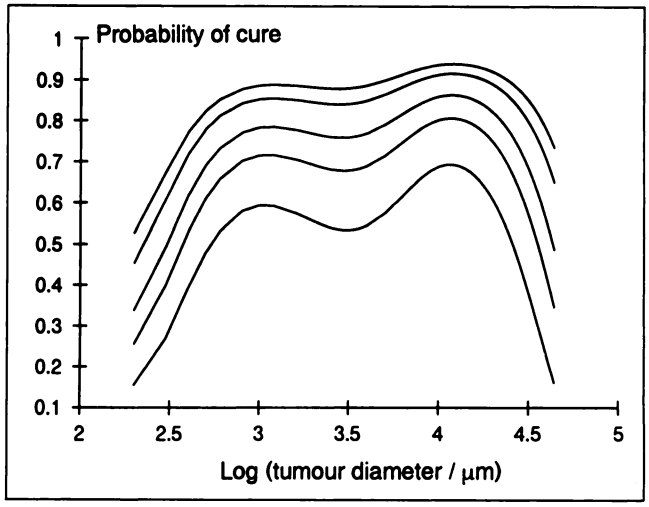

FIGURE 8. Possible relationship between tumor cure and tumor size for concurrent irradiation by radionuclides ^{199}Au and ^{90}Y. Combination of radionuclides of different optimal cure size may result in wider region of high curability.

Implications for Clinical Therapy

The calculations described above show that the physical characteristics of radionuclides are important determinants of their therapeutic usefulness. There is a range of tumor sizes in which a particular radionuclide is most appropriate. For the beta emitters considered here, this may be of submillimeter dimensions as for ^{199}Au, of several centimeters as for ^{90}Y or at some size range intermediate to these extremes. If it were known in advance that all tumors present in a patient were of a particular size, then it might be that a single radionuclide could be chosen for optimal therapeutic effect. This is unlikely, however, as there is usually a multiplicity of tumor deposits of varying sizes in patients with disseminated disease. Another important reservation is that the radionuclide distribution is not uniform. There are regions of relatively high and low uptake throughout tumors. If a long-range radionuclide (e.g., ^{90}Y) were to be used, then microtumors and metastases with dimensions of 1 mm or less would be resistant to treatment (as most of the disintegration energy will escape). Conversely, if a short-range emitter is used (e.g., ^{199}Au), cold spots, which experience a reduced dose and dose rate, could act as foci for tumor recurrence.

The implication of this argument is that the use of several radionuclides concurrently would be more effective than reliance on only one. A useful combination would require at least one short-range emitter and one long-range emitter. Short-range emitters would be included to deal specifically with smaller microtumors and metastases; long-range emitters would be included to deal with larger

tumors and to reduce the adverse effects of heterogeneity of radionuclide distribution. Figure 8 illustrates the principle of the use of two radionuclides in combination. In this case, the short-range emitter ^{199}Au and the long-range emitter ^{90}Y were used. By selection of appropriate activity ratios, the probability of tumor cure is kept at a more uniform level throughout the size range. This shows that, in principle, it is possible to extend the range of optimal curability. The concurrent use of multiple targeted radionuclides would appear to be an interesting topic for laboratory and clinical research.

A rationale for combination of targeted radionuclide therapy with XRT was previously discussed (*15,16*). This relies on XRT to eliminate tumor cells that have escaped sterilization by radionuclides. Either or both of local XRT and total body irradiation (TBI) may be appropriate, with elective bone marrow rescue being mandatory in the case of TBI. Clinical studies based on this strategy for treatment of advanced neuroblastoma with ^{131}I-MIBG, TBI and chemotherapy followed by bone marrow rescue are now in progress (*17*). As any tumor cells that escape targeted radiotherapy are likely to lead to recurrent disease, it would be anticipated that, even with the use of multiple radionuclides, integration with other therapeutic modalities, including XRT, would remain necessary to achieve a curative response.

CONCLUSION

The physical characteristics of radionuclides are important determinants of the tumor sizes for which the probability of achieving cure is maximized. With a mathematic modeling approach, it was found that there is an optimal tumor size for curability for each of 22 beta-emitting radionuclides of possible therapeutic potential. Optimal cure diameters extend from a minimum range of <200 μm to 1 mm for ^{33}P to a maximum range of 28 to 42 mm for ^{90}Y for uniform distribution of radionuclides throughout the tumor volume. The energy emitted per disintegration may be used as a predictor of optimal cure size.

ACKNOWLEDGMENTS

This work was supported in part by U.K. Medical Research Council grant G84/2436 and by grant 1083 of the Scottish Hospitals Endowment Research Trust.

REFERENCES

1. Lashford LS, Lewis IJ, Fielding SL, et al. Phase I/II study of ^{131}I metaiodobenzylguanidine in chemoresistant neuroblastoma—a United Kingdom Children's Cancer Study Group Investigation. *J Clin Oncol* 1992;10:1889–1896.
2. Hird V, Maraveyas A, Snook D, et al. Adjuvant therapy of ovarian cancer with radioactive monoclonal antibody. *Br J Cancer* 1993;68:403–406.
3. Press OW, Eary JF, Appelbaum FR, et al. Radiolabelled-antibody therapy of B-cell lymphoma with autologous bone marrow support. *N Engl J Med* 1993;329:1219–1224.
4. Riva P, Arista A, Tison V, et al. Intralesional radioimmunotherapy of malignant glioma: an effective treatment in recurrent tumors. *Cancer* 1994; 73:1076–1082.
5. Humm JL. Dosimetric aspects of radiolabeled antibodies for tumor therapy. *J Nucl Med* 1986;27:1490–1497.
6. Wessels BW, Rogus RD. Radionuclide selection and model absorbed dose calculations for radiolabeled tumor-associated antibodies. *Med Phys* 1984; 11:638–645.
7. Mausner LF, Srivastana SC. Radionuclides for radioimmunotherapy. *Med Phys* 1993;20:503–509.
8. Bardiès M, Chatal JF. Absorbed fractions of 22 potential beta-emitting radionuclides for internal radiotherapy. *Phys Med Biol* 1994;39:961–981.
9. Vatin R. *Programme SPEBETA. Laboratoire de Métrologie des Rayonnements Ionisants, internal report*. 1986.
10. O'Donoghue JA. The impact of tumor cell proliferation in radioimmunotherapy. *Cancer* 1994;73:974–980.
11. Fertil B, Malaise EP. Intrinsic radiosensitivity of human cells is correlated with radioresponsiveness of human tumors: analysis of 101 published survival curves. *Int J Radiat Oncol Biol Phys* 1985;11:1699–1707.
12. Steel GG, Wheldon TE. The radiation biology of paediatric tumors. In: Pinkerton CR, Plowman PN, eds., *Paediatric oncology: clinical practice and controversies*. London: Chapman and Hall; 1991:73–86.
13. Gaze MN, Mairs RJ, Boyack SM, et al. Iodine-131-metaiodobenzylguanidine therapy in neuroblastoma spheroids of different sizes. *Br J Cancer* 1992;66:1048–1052.
14. Bardiès M, Thedrez P, Gestin JF, et al. Use of multicell spheroids of ovarian carcinoma as an intraperitoneal radio-immunotherapy model—uptake, retention kinetics and dosimetric evaluation. *Int J Cancer* 1992;50: 984–991.
15. O'Donoghue JA. Optimal scheduling of combined biologically targeted radiotherapy and total body irradiation with bone marrow rescue for the treatment of systemic malignant disease. *Int J Radiat Oncol Biol Phys* 1991;21:1587–1594.
16. Amin AE, Wheldon TE, O'Donoghue JA, Barrett A. Radiobiological modelling of combined targeted ^{131}I therapy and total body irradiation for treatment of disseminated tumors of differing radiosensitivity. *Int J Radiat Oncol Biol Phys* 1993;27:323–330.
17. Gaze MN, Wheldon TE, O'Donoghue JA, et al. Multi-modality megatherapy with ^{131}I-meta-iodobenzylguanidine, high-dose melphalan and total body irradiation with bone marrow rescue: an innovative strategy for advanced neuroblastoma. *Eur J Cancer* 1995;31:252–256.